UCRL- 94419
PREPRINT

A Mechanistic Model for Axisymmetric UCG Cavity Growth

Charles B. Thorsness
Jerald A. Britten

This Paper was prepared for submittal to the: Twelfth Annual Underground Coal Gasification Symposium, August 25-28, 1986

July 1986

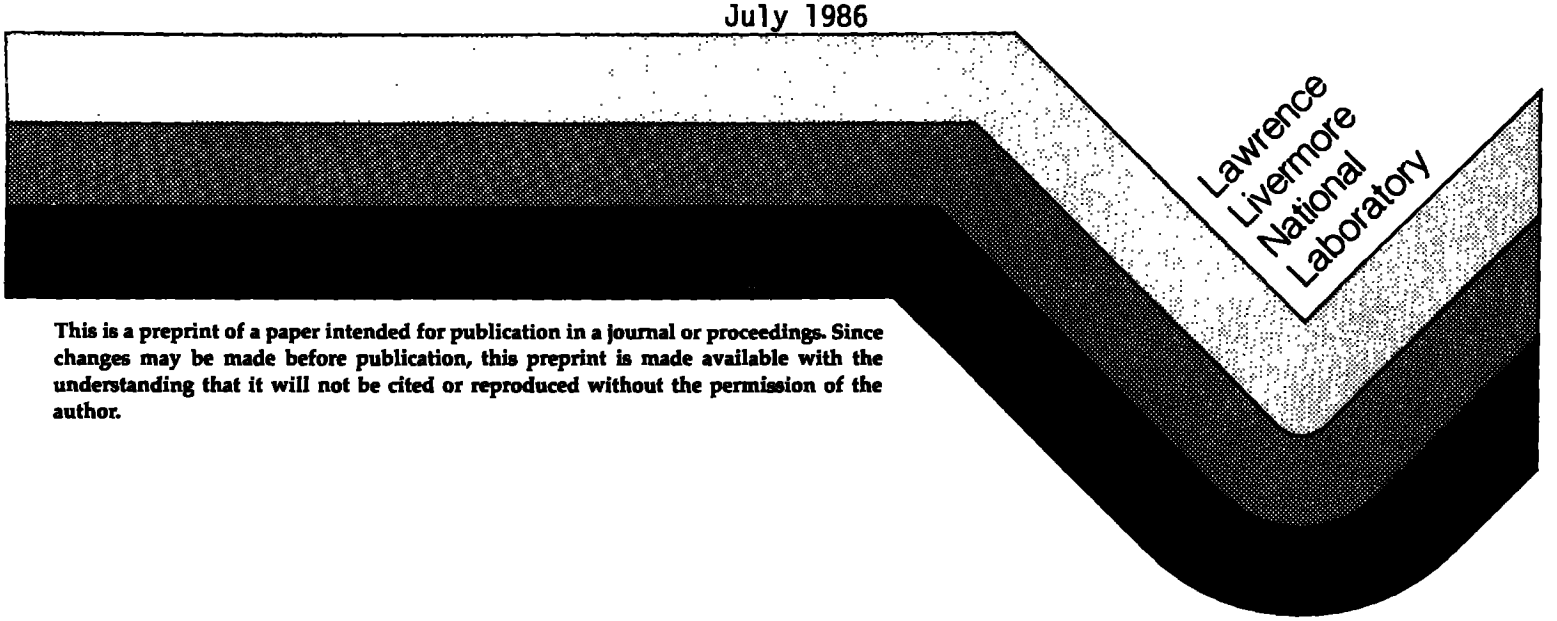

* A MECHANISTIC MODEL FOR AXISYMMETRIC UCG CAVITY GROWTH

Charles B. Thorsness 1/

Jerald A. Britten 1/

ABSTRACT

A three-dimensional, axisymmetric model to describe cavity growth during underground coal gasification (UCG) has been developed. The model makes use of a few basic assumptions concerning dominant heat and mass transfer processes in various zones of the cavity, and employs no arbitrary parameters of significant impact. Other features of the model include the capability to follow the evolution of the cavity from near start-up to exhaustion, and explicit coupling of wall and roof surface growth mechanisms. The model assumes the that cavity consists of up to three distinct rubble regions and a void space. Resistance to injected gas flow from a point low in the coal seam is assumed to be concentrated in the ash pile surrounding this point. A zone of relatively higher permeability is assumed to exist at the ash/coal wall interface, and rock and char rubble flow resistances are assumed negligible. Flow of injected gas through the ash is coupled by material and energy balances to cavity growth at the rubble/coal, void/coal and void/rock interfaces using previously developed submodels. The model is capable of simulating a wide range of coal and overburden compositions and stratigraphy, as well as water influx. In this paper, the model is described, the method of solution of the model equations is outlined, and the results of preliminary simulations are discussed.

INTRODUCTION

The size of the cavity formed during a UCG operation has a direct impact on economic and environmental considerations crucial to its success. The lateral dimensions of the cavity determine module spacings along a horizontal drilled link and lateral distances between drilled links, and overall cavity dimensions determine hydrological and subsidence behavior of the overburden. Mathematical modeling can be an invaluable predictive tool for determining the effects of geologic, coal property and process variables on cavity growth dynamics during UCG, and in the last ten years considerable effort has been devoted to development of such models. Descriptions of these models can be found in the various UCG Symposia Proceedings, published annually since 1975, and reviews of many of the models developed are available (Riggs and Edgar, 1983; Kunselman et. al., 1983). Formulation of an adequate cavity growth model is a difficult problem which requires considerable expertise in a number of technical areas including rock mechanics, fluid flow, heat and mass transfer, chemical kinetics and hydrology. Also, fundamental mechanisms for cavity surface recession, in particular rubblization phenomena of consolidated coal and rock surfaces subjected to heat, are not as yet well understood. For these reasons none of the cavity growth models to date, including more comprehensive latter ones (Thorsness and Cena, 1983; Chang et. al., 1984), are predictive, since they rely to some extent on one or more of the following: arbitrary assumptions or parameters to control oxidant flow distribution in the cavity; oversimplification of some crucial phenomena done to allow detailed treatment of others; or boundary conditions on upward or outward growth, either arbitrarily chosen or fitted a-posteriori from field data, which uncouple cavity surface recession rates from heat and mass balance constraints.

It is the challenge of the modeler to formulate mathematical descriptions of UCG cavity growth which are tractable within current computational resources, but which retain sufficient physics to adequately describe the process with a minimum of adjustable parameters. The model must also be made versatile enough to be used for a variety of conditions, so that its predictive capability be maximized. To this end, dominant forces controlling cavity growth must be identified and incorporated. Any symmetry, either geometrical or thermophysical, which exists in the system must be found and exploited to simplify the formulation.

The model described in the following sections is a step, we would hope, toward these objectives. It is currently being refined, but the basic structure has been completed

1/ Lawrence Livermore National Laboratory, Livermore, California USA

and exercised. The main features of the model are that it contains no adjustable parameters of significant impact, but instead relies on a few basic assumptions concerning heat and mass transfer processes occurring at different locations within the cavity. Cavity surface recession rates are mechanistically calculated by energy and material balances, in terms of postulated failure criteria for the coal and rock overburden. The model is capable of simulating cavity growth over virtually the entire life of a UCG module. Growth mechanisms are allowed to change smoothly as the system evolves from a small, relatively empty cavity low in the coal seam to a large, almost completely rubble-filled cavity extending high into the overburden rock. The model is general enough to treat any type of coal or overburden, coal seam thickness, multiple overburden layers, and almost any injection gas flow schedule and composition. Its modular nature provides for straightforward addition of optional submodels. Provision for water influx, based on a specified permeation flux per unit area of the cavity, is included.

A series of schematics of cavity configurations envisaged by the model is shown in Figure 1. Axisymmetric growth about an injection point assumed to be at the bottom of the coal seam is considered. This is done to allow the treatment of the three-dimensional growth in terms of two dimensions, r and z in cylindrical coordinates, and therefore the model is perceived to represent the actual full-seam consumption volume of the coal seam. At present, an outflow channel is not modeled. Inclusion of an outflow channel model as a submodel to describe additional coal drying, charring and the associated gas production is straightforward, but actual physical inclusion of an outflow channel in the global model would break the symmetry enjoyed by the present formulation and require a formidable, fully three dimensional solution. Axisymmetry about the injection well has been assumed in previous cavity growth models (Krantz et. al., 1980; Gibson and Wheeler, 1980). Furthermore, examination of coring data from the Hoe Creek II (Aiman et. al., 1980) and Hanna II phases 2 and 3 Youngberg and Sinks, 1981) UCG field tests, and preliminary excavation data coupled with coring data (Dana, et. al., 1986) for the Partial Seam CRIP UCG test suggest that the boundary of full seam consumption of a UCG burn can be quite reasonably represented by an axisymmetric cavity centered at the injection point, since back- and side-burning of the cavity occur to about the same extent, and a large portion of the affected coal extending down the link to the production well consists of a narrow charred outflow channel, not a true cavity.

The cavity is considered to consist of up to three distinct rubble zones composed of ash, char and rock rubble, and a void space at the top. A fundamental assumption is that all resistance to injection gas flow occurs in the ash rubble pile. A thin zone of relatively high permeability is assumed to exist at the ash pile/coal wall interface, attracting injection flow to the outer edges of the ash pile, where it reacts with char and drives lateral growth. This assumption is the basis for a wall recession submodel (Grens and Thorsness, 1986) used in the global model. Mechanisms explaining the existence of a high-permeability zone near the wall have been proposed for deep, thin seams (Wilks, 1983), but for general cases this assumption has yet to be verified. The rock and char rubble overlying the ash are assumed to have much lower resistances to gas flow. With these assumptions, determination of the injection gas flow distribution amounts to calculation of flow through the ash rubble only. This injection flow arrives at three distinct regions defining the outer edge of the ash pile: the wall, defined as the ash/coal interface; the outer bed, defined as the char rubble/ash rubble interface; and the inner bed, defined as the ash/void or ash/rock rubble interface. Oxidant flow to the wall determines its local recession rate, and oxidant flow to the inner and outer beds drives recession of the remaining cavity surfaces.

Another symmetry by which considerable simplification can be realized is found in the chemical reactions that dominate the cavity growth. If methanation reactions are neglected as secondary contributors to the cavity growth process and a lumped gas-phase system is defined as consisting of species O_2, $A = H_2O + CO_2$ and $B = H_2 + CO$, chemical reactions responsible for cavity growth become:

$$O_2 + C \rightarrow A + q_1 \ , \qquad (1)$$

$$A + C \rightarrow 2B + q_2 \ , \qquad (2)$$

$$O_2 + 2B \rightarrow 2A + q_3 \ . \qquad (3)$$

Heats of reaction for reactions 2 and 3 (or equivalently heats of formation of species A and B) are weighted averages of those for the constituent species based on the composition of the injected gas. Detailed product gas compositions can be obtained from calculated production rates of species A and B by use of water-gas shift reaction equilibrium at the product gas temperature. This simplified reaction scheme has been used in models (Britten and Thorsness, 1986; Grens and Thorsness, 1986), employed as modules in this global simulator, and a discussion and justification of this reaction scheme can be found in the former reference. Since combustion reactions are assumed to be rapid and to go to completion, the only kinetic rate considered in the model is for the endothermic gasification reaction (2), assumed to be given by steam/char reaction kinetics.

Convective heat transfer is assumed to be the controlling mechanism supplying heat to the competent coal sidewalls in the rubble regions, while radiative transfer dominates in the void region. The void is assumed to be well-mixed, such that gas-phase combustion of product gases occurs at a thin flame sheet at the ash/void or rock rubble/void interface. Surfaces enclosing the void are assumed to be black, although extension to consider gray surfaces would

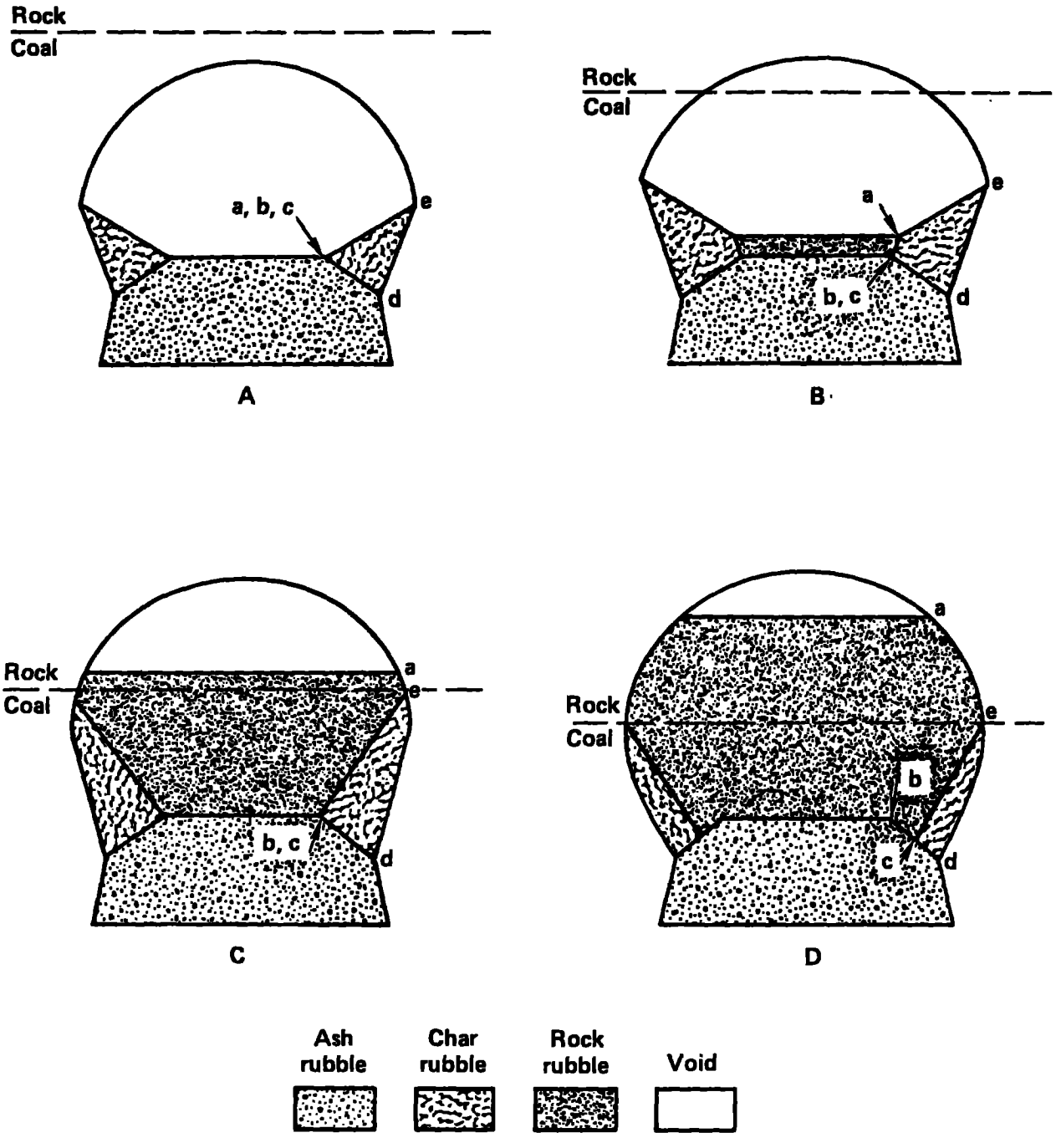

Figure 1. General cavity shapes considered by the model.

be straightforward, and the medium is assumed transparent to radiation. For typical cavity temperatures convection in the void, which can be modeled in terms of a mixed-mode heat transfer coefficient not readily estimated, has been shown to contribute only a small portion of the heat flux to the void boundaries compared with radiative transport (Britten and Thorsness, 1986). Also, it has been shown (Britten, 1985) that absorption of radiation by H_20 and CO_2 in the void gases results in a quite minor adjustment in heat fluxes and surface recession velocities, such that the assumption of radiative transparency of the void is justified, as long as significant scattering by ash and soot particles does not occur.

In the following sections, submodels used in the development of the global cavity growth model are introduced, and the solution algorithm used to couple these submodels is discussed. Results of calculations to determine numerical sensitivity are then discussed, followed by a preliminary comparison of model predictions with field data.

MODEL FORMULATION

Injection Gas Flow Submodel

At any instant the flow through the ash rubble is quasi-steady, since the evolution of the ash pile is on a much longer time scale than the residence time of the flow through it. The flow distribution is obtained by solving the compressible Darcy flow equation, written in cylindrical (r,z) coordinates:

$$\frac{\partial^2 P^2}{\partial z^2} + \frac{1}{r}\frac{\partial}{\partial r}\left(r\frac{\partial P^2}{\partial r}\right) + \frac{2RT\mu}{\kappa}\Omega = 0 \ , \qquad (4)$$

The source term Ω is nonzero only at the origin r,z=0. Boundary conditions are:

$$(r = 0) \quad \frac{\partial P^2}{\partial r} = 0 \quad \text{(symmetry)} \qquad (5a)$$

$$(z = 0) \quad \frac{\partial P^2}{\partial z} = 0 \qquad (5b)$$

(impermeable cavity floor)

$$(r = \Psi(z)) \quad P^2 = P^2_{sink} \qquad (5c)$$

(along upper and side ash pile boundaries)

A finite difference algorithm is used to solve equation (4). Half of a cross section of the axisymmetric ash pile is mapped onto a m x n grid, rectangular in r and z coordinates, and scaled in such a way as to maximize the number of nodal points lying inside the ash pile boundary. Permeability values for nodal points lying outside the boundary are given very high values, effectively tying the edge of the ash pile to the sink pressure. The difference equations resulting from discretization of eqn. (4) are written for each nodal point, and pressures at these nodes are then calculated by direct solution of the linear system in P^2. The injection source is averaged over the volume of the first grid region centered at the origin. Given the solution for the field variable P^2, fluxes at each edge surface are then computed. Due to the discretization, fluxes at the boundaries are not smooth, but exhibit spikes and troughs at points where the ash pile boundary is not parallel in r or z. Therefore, the fluxes are smoothed by fitting a 3rd order polynomial to the computed values, and the integrated flow over the entire boundary is renormalized with the injection flow to remove slight errors in the mass balance resulting from the smoothing operation. Total flowrates to the wall, outer and inner bed surfaces are then calculated for use as input variables for the cavity growth submodels. The rectangular grid is rezoned and the flow solution recalculated at each time step.

Wall Submodel

The wall layer is assumed to be a thin, highly permeable layer of char and ash separating the inert ash rubble of the main cavity from the coal at the wall. A model of this wall layer has been developed (Grens and Thorsness, 1986) in which effects drying and pyrolysis of the coal wall, and combustion and gasification of char were combined to yield a solution for the quasi-steady wall regression rate and and produced gas composition and temperature. It was found that computed results were predominately determined by the oxygen flux to the layer. This model assumes, in effect, horizontal motion of the ash to replace matter removed by char combustion in the reaction zone. In the framework of the present global model, it is more natural to consider downward motion and subsequent reaction of char from the outer char bed to fill the void left by removal of carbon from the wall. Work is currently underway to extend the wall layer model to treat the case of vertical char motion, but in the meantime a simpler submodel has been incorporated which we believe captures the essential features of this phenomenon. Simplicity is achieved by the introduction of two parameters not present in the more complete model, a prescribed extinction temperature and an energy transport parameter. These parameters will not be required when the more complete wall model becomes available.

A schematic of the wall layer model is shown in Figure 2. Quasi-steady translation of this reactive layer from left to right into the coal is assumed. In a coordinate system moving with the wall layer, the injected gas enters a differential slice of the control volume from the left; char, water vapor and pyrolysis gas enter from the right, driven by a conductive heat flux into the coal; char rubble from the outer bed settles from above; ash exits from the left and product gases exit the top of the slice. Only the gas flow rate is allowed to vary axially along the wall layer. This allows the discretization of the wall layer into segments lying atop each other. The final product gas flow rate is computed by summing over the segments.

The parameters are introduced into the model by dividing the layer into two subzones, one in which gasification of the char occurs and one in which the wet coal is dried and

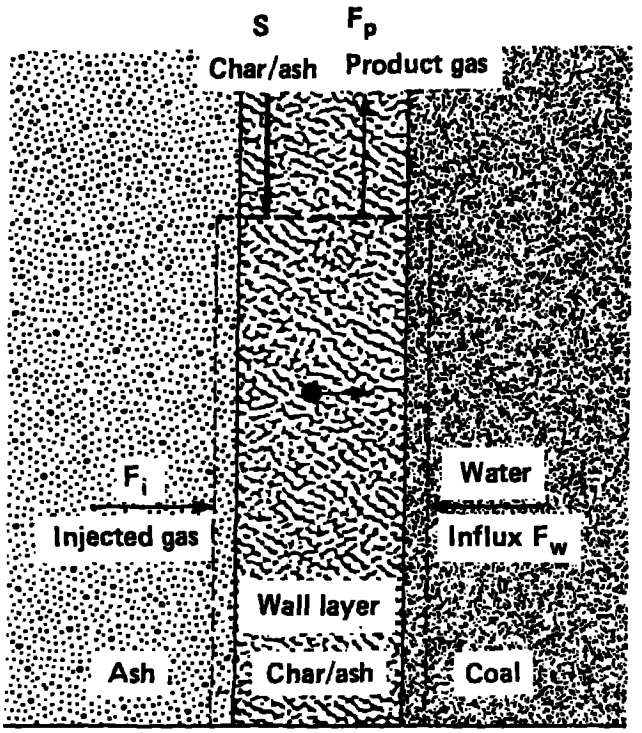

Figure 2. Schematic of reactive wall layer submodel.

pyrolyzed. Figure 3 shows this division, in which zones I and II comprise the combustion/gasification and drying/pyrolysis regions, respectively. A specified extinction temperature for the steam/char reaction determines the temperature boundary between the subzones. The other parameter is a measure of the relative contribution of convection and conduction to the transport of energy from the gasification subzone to the drying and pyrolysis subzone. It is set equal to zero if all energy needed to drive the wall pyrolysis and drying comes from sensible heat in the hot gases convected from the gasification zone, and to one if this heat is removed from the gasification zone only by conduction.

Energy balances for zones I and II are written:

$$Sh\big|_{T_s} + F_i h_i\big|_{T_i} + S_{ch}h_{ch}\big|_{T_p} = S_a h_a\big|_{T_s} + F_r h_r\big|_{T_s} + Q_l , \quad (6)$$

$$F_r h_r\big|_{T_s} + Q_l + F_w h_w\big|_{T_-} + S_c h_c\big|_{T_-} = S_{ch}h_{ch}\big|_{T_p} + F_p h_p\big|_{T_p} . \quad (7)$$

(Symbols in the above equations are defined in the nomenclature section). The final energy balance is used to define the value of Q_l used above. It involves a balance around zone II assuming the gas stream F_r is zero and that the gas produced by drying and pyrolysis emerges at the extinction temperature. The balance is used to define Q, the amount of heat necessary to dry and pyrolyze the coal and heat all products to the extinction temperature, given by:

$$Q = F_v h_v\big|_{T_s} + S_{ch}h_{ch}\big|_{T_s} - F_w h_w\big|_{T_-} - F_c h_c\big|_{T_-} . \quad (8)$$

The value of Q is then used in the simple relation:

$$Q_l = x_t Q \quad (9)$$

to give Q_l as a function of the heat transfer parameter x_t.

The following mass balance on ash is used to define the magnitude of the solid stream S:

$$v\rho_a + w_a^* S = v\rho_s w_a \quad (10)$$

The char stream S_{ch} leaving zone II and entering zone I is given simply by:

$$S_{ch} = (1 - w_w - w_v)S_c \quad (11)$$

Gases produced by drying and pyrolysis are combined with reaction-created gas F_r to give the produced gas flow F_p:

$$F_p = (w_w + w_v)S_c + F_w + F_r . \quad (12)$$

The resolution of w_v into various constituent species according to our simplified chemical species formulation requires data on representative amounts of CO, CO_2, H_2, H_2O and hydrocarbons which are formed from the coal volatile matter under UCG conditions.

The amount and composition of stream F_r is found by using balances for each gas component which include the rates of species production in zone I. Complete consumption of oxygen by gas-phase combustion of B-gas is assumed. Therefore, the net production rate of B-gas is:

$$\frac{d[B]}{dt} = 2S_{ch}\frac{w_c}{w_c + w_a} - 2Y_{O_2}F_i , \quad (13)$$

Finally, the net rate of A-gas production is given by;

$$\frac{d[A]}{dt} = -S_{ch}\frac{w_c}{w_c + w_a} . \quad (14)$$

The coupling of the above set of equations requires an iterative solution scheme to be employed to determine the primary unknown v.

As described earlier, we have assumed that the void created at the wall by the conversion of carbon will ultimately be filled by ash from two sources, from local coal and from the char which settles from above to fill the developing void. The ash content of most coals dictate that the amount of settling char is higher than the amount of char removed from the wall. Since this char is already heated, it has the effect of making the model fairly insensitive to the exact values of the wall parameters used.

Roof/Rubble Zone

The roof/rubble bed region consists of the char and rock rubble piles and the surfaces that comprise their boundaries, and the surfaces enclosing the void region of the cavity. The roof is defined as the coal/void or rock/void interface. Roof surfaces are required to have a positive radius of curvature at all points with respect to the center of the void. Thus, the problem of shadowing, which complicates the radiative exchange calculations, is avoided.

The roof surface is divided into n segments, one a disk or cone at the apex of the cavity and the remainder

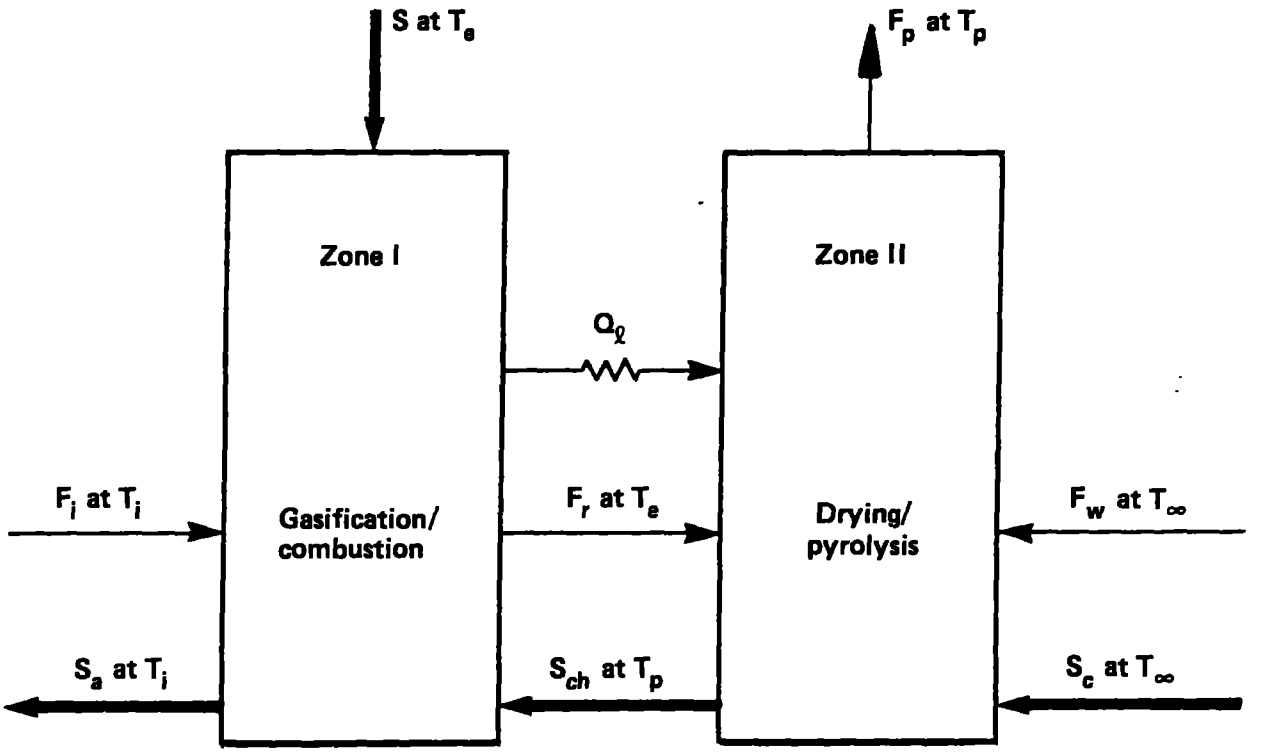

Figure 3. Control volume representation of reactive wall layer model, defining streams for mass and energy balances.

axisymmetric rings extending down to the top of the char rubble pile. The assumed spalling/surface renewal mechanism allows for treatment of the recession of each segment as locally one-dimensional, since the thermal penetration thickness into the coal or rock is thin compared with the dimensions of the cavity. For given coal/rock composition, failure parameter values and water influx values, total recession rates (spalling plus gasification), spalling rates, heat fluxes and evolved gas fluxes and compositions are calculated for a range of heat source temperatures by use of a one-dimensional transient spalling/gasification model (Britten, 1986; Britten and Thorsness, 1986) and tabulated as functions of the mean roof surface temperature, averaged over a number of spalls. This tabulated data is used in the global model. In this fashion, the recession characteristics of each roof segment are unique functions of its surface temperature, which is an unknown to be determined by solution of the radiative exchange equations. Provision for multiple recession rate data tables for coal or rock is included, such that recession characteristics can be made angle dependent, for example.

For calculation of the radiative exchange view factors between the surfaces enclosing the void, imaginary disks are constructed at the endpoints of each ring segment comprising the cavity boundary. By use of the formula for coaxial disk-to-disk view factors (Shapiro, 1983), view factors between cavity surface segments can be calculated using view factor algebra for a black enclosure (cf. Siegel and Howell, 1981). The net radiative heat transfer at surface j is to be balanced by the mean conductive flux into the surface, $\hat{Q}_j$:

$$\hat{Q}_j(T_j) = \sigma A_j T_j^4 - \sigma \sum_{k=1}^{n} A_k f_{jk} T_k^4 \ . \qquad (15)$$

For the moment we consider the case in which overburden rock has not yet been exposed, and thus no rock rubble exists in the cavity (Figure 1a). Results of a preliminary study using a model with a single flat rubble bed on which char particles fell directly from above showed a tendency for char to accumulate at the outer edges of the rubble bed, and for substantial amounts of oxygen to pass unconverted from the ash pile into the void near the center of the rubble bed. This is because the system geometry dictates that oxygen flux is higher near the center of the bed, while the area ratio of roof surface to underlying rubble surface increases away from the cavity center. Thus, the ratio of oxygen rates to char rates falls off significantly with distance from the cavity center. For this reason the rubble/void interface is divided into two zones, an inner bed on which char does not accumulate but reacts completely with oxygen and steam injected from below, and an outer bed in which char can accumulate. The angles of the char bed/void and char bed/ash bed interfaces are specified. Local equilibrium of gas and solid temperatures in the rubble zones is assumed.

Char enters the outer char bed by spalling from above, and by rubblization of the coal sidewall adjacent to the char pile, according to a wall recession mechanism proposed by (Grens and Thorsness, 1985). Char is

removed from this bed by: settling along the coal sidewall to react with oxygen and steam in the wall layer as discussed previously; by reaction with oxygen and steam entering below from the char/ash interface; and by rolling off of a fraction of the spalled material onto the inner bed, where it is consumed by reaction. The amount of char spalling onto the outer bed which rolls off into the inner bed is calculated, not specified, and is a key variable for early cavity growth.

Since the length of the active reaction and gasification zone in a packed bed of coal is relatively thin, on the order of a few tens of centimeters under typical conditions, the gasification zone at the bottom of the char pile adjacent to the char/ash interface is modeled as a one-dimensional packed bed based on the char/ash interfacial area. Oxygen entering from below combusts, and above this combustion zone steam and carbon dioxide gasify the coal. These endothermic reactions occur until the char bed temperature reaches the extinction temperature of the steam/char reaction T_e, which can be calculated by the asymptotic formula given in (Britten and Thorsness, 1986) in the limit of a large activation temperature. Char conversion in this zone is then analytically calculated as a function of this temperature. Convective heat transfer from the hot product gases at Te to the coal wall causes this wall to rubblize and recede as a function of a failure temperature parameter T_f (Grens and Thorsness, 1985). This rate of recession is quite small compared with the radiation-driven recession rates of the roof surfaces above, and for practical purposes the cavity ceases to grow as the sidewalls become covered with char rubble. Nevertheless, this recession rate is calculated. This is a quasi-steady process again, since the sidewall recession rates are much smaller than the gas flowrates. The drop in gas temperature by convection to a sidewall of length L and area A at a temperature of T_f is given by solution of:

$$F_{ob}C_g\frac{dT}{dz} = H(T - T_f) \ . \qquad (16)$$

with the boundary condition $T(z=0)=T_e$. The (trivial) solution to this is integrated to find the mean temperature $\langle T_{ob}\rangle$ of the char bed, and this in turn is used to calculate the recession velocity of this surface:

$$\frac{HA}{L}(\langle T_{ob}\rangle - T_f) = A\bar{Q}v \qquad (17)$$

where $\bar{Q}$ is the heat required to dry and char a unit mass of coal from ambient temperature to $\langle T_{ob}\rangle$.

Finally, the free surface of the outer char bed adjusts to a radiative equilibrium determined by the temperatures of the other surfaces enclosing the void. Thus, a thin layer near this surface exists wherein the gas is raised (or lowered) to T_{ob}, as described by the following equation:

$$F_{ob}C_g(T_{ob} - \langle T_{ob}\rangle) = \sigma(A_{ob}T_{ob}^4 + \sum_{k=1}^{n} f_{ob,k}A_kT_k^4) \ . \qquad (18)$$

We define α as the fraction of char spalled onto the outer bed which subsequently rolls onto the inner bed. A mass balance on the char is needed to determine this variable. If S_1 is the spalling rate to the outer bed, S_2 is the rate at which char settles into the wall region, S_3 is the char addition rate by rubblization of the sidewall and S_4 is the char gasification rate at the bottom of the bed, then:

$$\frac{d(char)}{dt} = (1-\alpha)S_1 - S_2 + S_3 - S_4 \ . \qquad (19)$$

The inner bed surface provides the bulk of the heat needed to drive recession of the roof surfaces. It is assumed that char does not accumulate here, but gasifies at the rate $S_t = S_{ib} + \alpha S_1$ at which it enters. An energy balance at this surface relates the temperature of this surface to α and the temperatures of the other surfaces enclosing the void. The general form of the energy balance at this surface is;

$$\sigma(AT_{ib}^4 - \sum_{k=1}^{n} A_k f_{ib,k} T_k^4) + S_t C_s(T_{ib} - \langle T_{prt}\rangle) +$$

$$(F_{ib}C_g - S_t w_a^* C_a)(T_{ib} - T_f) = \min\left[\frac{S_t w_c^*}{M_c}, F_{ib}Y_{O_2}\right]q_1 + \qquad (20)$$

$$\max\left[\left(\frac{S_t w_c^*}{M_c} - F_i Y_{O_2}\right), 0\right]q_2 + \max\left[\left(F_i Y_{O_2} - \frac{S_t w_c^*}{M_c}\right), 0\right]q_3 \ .$$

Solution Algorithm

The injection flow distribution to the wall, outer and inner bed regions is calculated for a given ash pile geometry, and bulk densities for the ash, char and rock rubble are specified. For α fixed, the system of n+2 nonlinear equations, n of the form of eqn. (15) for the roof surfaces, along with eqns. (18) and (20), are solved simultaneously by Newton iteration to determine the temperatures of all surfaces enclosing the void. Wall recession rates and char and ash addition rates from the wall model, and char and ash addition rates from the inner and outer bed regions become known as functions of α. The vertical growth rate of the ash pile is a function of α as well. Therefore, once a solution for a given α is obtained a tentative time step is taken, cavity boundaries are advanced, and new ash and char amounts are calculated. The height of the ash pile is fixed, and the ash balance is used to determine the radial position of point b of Figure 1A. In general, this position will not satisfy the char balance, and so α is adjusted using a golden section scheme, and variables are recalculated as described above, until both ash and char mass balances are satisfied and thus a solution for the new cavity shape obtained.

When the cavity grows to encompass overburden rock, as in Figures 1B-D, the solution algorithm becomes more complex. Two possibilities are allowed to exist. One demands that α=0, and thus upward growth of the ash pile is halted. In this case, oxygen passing through the inner bed combusts product gas at the top of the rock rubble pile. Surface temperatures, ash and char addition rates are calculated, and a tentative time step is taken. An ash

balance determines the position of point b, and rock and char balances solved simultaneously determine the coordinates of point a (Figure 1B). The radius of point a is constrained to be no smaller than that of point b. If the mass balances require $r_a < r_b$, r_a is set to r_b and α is freed from its zero constraint and allowed to adjust to satisfy the mass balances under these conditions. The philosophy here is that char overlying the inner bed from which injected gas is issuing is attacked and removed by oxygen and steam, while it is more or less insulated from these gases when the angle of repose of the char/rock interface, relative to the to inner bed surface, is greater than 90°, as in Figure 1B.

As the cavity continues to evolve, rock rubble can completely cover the char rubble, as in Figure 1C. In this case, the rock balance determines point a, and point e remains at or near the coal/rock boundary. The relatively slow char addition rates to the outer bed due to sidewall decrepitation are generally not sufficient to offset char removal by gasification at the bottom of the char bed. Thus, char begins to disappear later in the simulation, and this situation is handled by allowing point c to adjust to satisfy the char mass balance (Figure 1D).

To calculate cavity growth for a given time step, surface velocities on each side of a cavity point are averaged by area weighting, and this point moved outward a distance v Δ t in a direction determined by the angle bisecting the angle defined by the adjacent surfaces. Adjacent points may move at significantly different velocities, such that some segments of the roof enclosure evolve a negative radius of curvature with respect to the center of the void. Since this is not allowed by the radiative exchange calculation, an algorithm is invoked at each time step to adjust point locations as necessary to assure a positive radius of curvature between all segments of the roof enclosure. Also, in regions of slow growth, points tend to cluster together. Thus, at selected intervals a point equalization algorithm is exercised to redistribute the points equally along the cavity boundary. Each of these "smoothing" algorithms introduces an error in that the resulting cavity volume may not agree with the original volume. These errors are accumulated and printed at each time step, and it has been found that for a sufficient number of cavity points, this cumulative volume error does not amount to more than 2-3%.

A cavity growth simulation is begun with a small cavity of a prescribed initial size, shape and char capacity. The simulation proceeds and the cavity passes through the various stages of evolution shown in Figure 1. The simulation is terminated when the end time is reached, the concentration of "B" gas in the product stream goes to zero, the char becomes completely consumed or the rock rubble bulks to fill the entire cavity. The solution algorithm is relatively stable, but certain pathological cases do arise in which instantaneous mass and energy balances cannot be satisfied within the imposed constraints, and the simulation halts. These cases are relatively uncommon, specific to details of the input parameters, and are in many cases related to the smoothing algorithms. Usually, the simulation can be restarted by accepting the error occurring at this time step, and will continue with no further problems. Thus, it is not felt instructive to discuss specific cases here.

RESULTS AND DISCUSSION

A base case consisting of generic coal and rock properties, operating and numerical parameter values given in Table 1 has been formulated and used in the simulation for illustrative and comparative purposes.

Table 1

Physical and parameter values used in base case simulation.

coal density: 1350 kg/m^3
coal composition: $w_c = 0.4$, $w_w = 0.2$, $w_a = 0.1$
rock density: 2100 kg/m^3
rock composition: $w_w = 0.12$
coal failure parameters: $T_f = 700$ (K), $l_f = 0.01$ (m)
rock failure parameters: $T_f = 1000$ (K), $l_f = 0.02$ (m)
rubble densities: char=800, rock=1300, ash=800 (kg/m^3)
wall parameters: $T_e = 1000$(K) , $x_t = 0.5$
injected gas composition: $Y_{O_2} = 0.33$ $Y_{H_2O} = 0.67$
21 cavity points
angles of char bed surfaces: $\gamma = -0.65$ $\omega = 0.5$ (radians)
21 x 21 matrix for flow calculation through ash
$\Delta t = 1.3 \times 10^4$ (s)
smoothing frequency: every 4 time steps

Figure 4 shows the development of the simulated UCG cavity for these conditions at six time intervals. An initial size, shape and unreacted char volume (Figure 4A) is assumed at zero time. As is shown in Figure 4B, the cavity grows smoothly in all directions while in the coal seam; the relative rates of lateral and upward growth remain relatively constant, and the amount of unburned char increases in proportion to the entire cavity volume. This simulation considered the spalling characteristics to be independent of the orientation of the coal/void interface, but assumed a much stronger overburden than the coal, such that upward growth of the cavity becomes severly retarded as it penetrates into the overburden (Figure 4C). Cavity temperatures increase only slightly during this mode of growth because coal remains a large fraction of the surface enclosing the void; coal surfaces in the void recede rapidly compared with other surfaces at this time. The ash pile controlling the gas flow distribution ceases to grow upward, and as a result the lateral growth slows as the coal wall boundary moves away from the injection gas source, and the fraction of oxidant exiting the top of the ash bed continues to increase. This oxygen combusts product gas in the void,

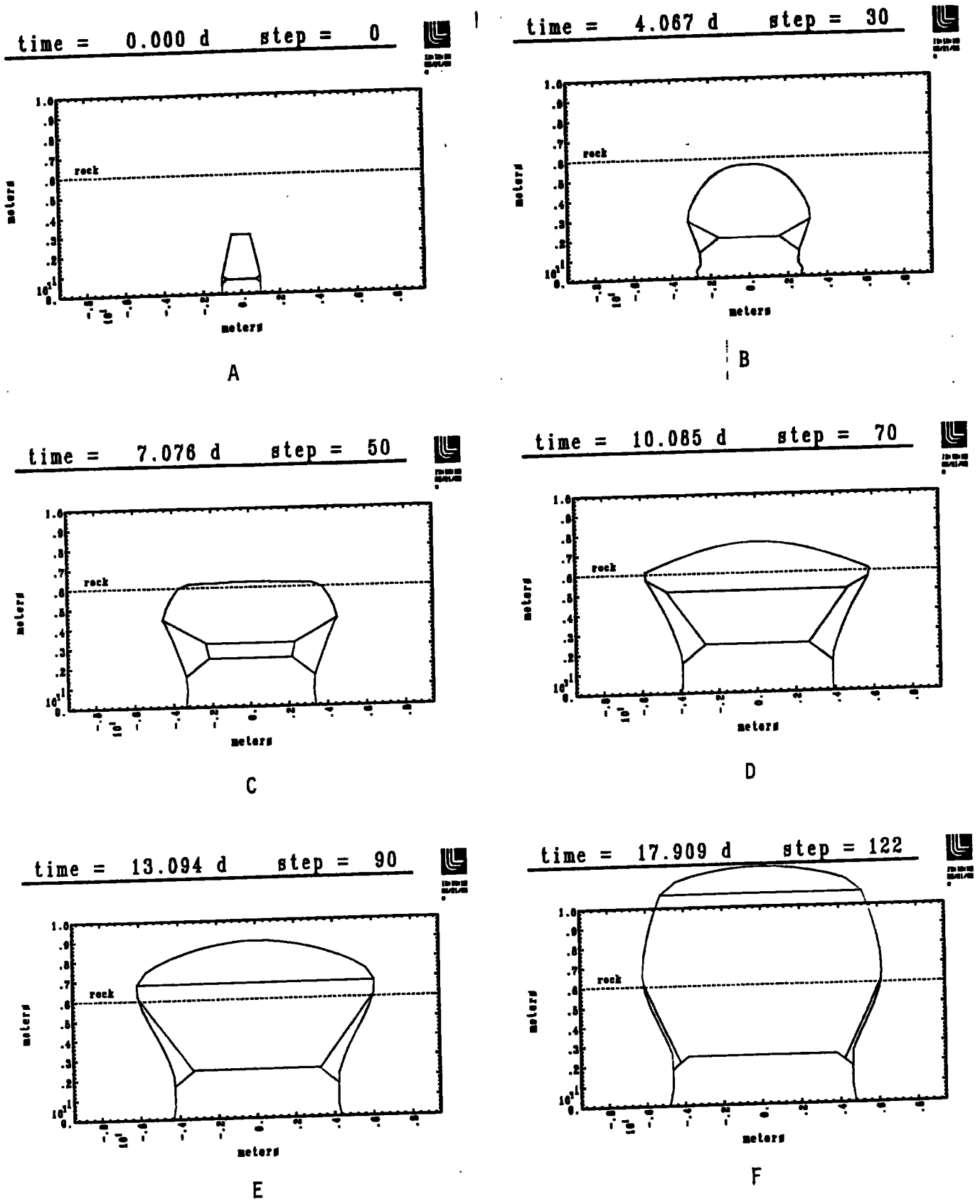

Figure 4. Calculated cavity shapes for the base-case simulation, at six different times.

eventually raising the temperature sufficiently to renew upward growth into the rock (Figure 4D). At this time the amount of unburned char remaining in the cavity begins to decrease. Comparison of Figures 4C,D and E show that lateral growth virtually ceases as the wall becomes covered with rubble. Eventually, production of combustible gas fails to convert all of the oxygen bypassing into the void, and the simulation is ended (Figure 4F). Recovery of unconverted oxygen rarely occurs in real systems, and two effects can be incorporated into the model to extend the life of the simulated process. Addition of an outflow channel for conversion of the oxygen will give more realistic gas production rates for the late life of the burn. Also, it is probable that the flow resistance of the rock rubble cannot be ignored when this rubble begins to fill a large fraction of the cavity. If this is the case, some oxygen will begin to be be diverted to the sidewalls to convert coal, resulting in more lateral growth. The value of the relative permeability between the rock and ash rubble would of necessity be rather arbitrary, however, in light of the fact that no data exist on in situ rubble permeabilities. For this reason, this effect has not been explored.

To be useful as a predictive tool, a global cavity growth simulator must give results relatively free of the influence of arbitrarily adjustable or numerical parameters. A series of simulations were performed in which parameters were systematically varied from the base case. A description of these simulations is given in Table 2, and results are shown in Table 3. An increase in the maximum time step by a factor of eight results in a difference in total cavity volume and combustible gas production of 6%, while increasing the computational time by a factor of 3.3. The cavity size increases as the time step increases, but this is localized in the overburden volume; the volume of affected coal is almost independent of time step. An increased frequency of point equalization decreases the cavity volume, with the effect more pronounced at high frequencies. Again, the error introduced by this smoothing is almost entirely concentrated in the overburden. Although neither error is substantial within the confidence limits of the model, it appears that an increase in computational efficiency can be realized by using larger time steps, and employing point equalization more frequently to compensate for the error involved.

The computational time increases dramatically with the number of cavity points used in the simulation, so a compromise must be reached between accuracy and cost. Simulations have shown that 21 cavity points give a result for cavity volume within 5% of that when 31 cavity points are used, and use a third of the computer time. The number of nodes used in the calculation of the flow through the ash rubble also has a significant impact on the computation time, but it is very important to obtain an accurate solution for this flow, since the distribution of oxygen to the various zones contacting the ash rubble plays a dominant role in the cavity development. It was found that for the most pathological cases studied, a grid size of 31x31 gave a solution of sufficient accuracy.

Table 2

Description of simulations investigating numerical parameter sensitivity. Lists change from base case conditions of Table 1.

run	change
num.0	base case
num.1	$2x\Delta t$
num.2	$4x\Delta t$
num.3	$1/2x\Delta t$
num.4	point equal. every step
num.5	point equal. every 10 steps
num.6	$\gamma = -0.46$
num.7	$\gamma = -0.81$
num.8	13 cavity points
num.9	31 cavity points
ini.1	$r_0 = z_0$, same initial vol.
ini.2	$r_0 = z_0/3$, same initial vol.

The effect of initial shape was also investigated in two simulations begun with right-circular cylindrical cavities of the same volume, differing in height by more than a factor of two. These simulations gave combustible gas production totals that differed by 9%, certainly within the confidence limits for the predictive capabilities of a model of this type.

The angle γ defining the position of the ash/char rubble interface appears to have the largest effect of any pure parameter on the outcome of the simulation. Two simulations were performed with values for γ of -26^0 and -46^0, measured from the horizontal inner-bed surface. Results of these simulations differed in the amount of produced combustible gas by about 15%. While this is not a dominating effect, it would be desirable to reduce it. The general ash pile geometry of Figure 1 was chosen as the simplest representation of an ash rubble zone that intuitively is felt to propagate stably outward as a smooth surface about the injection source, due to the way in which ash is formed locally in direct proportion to the amount of oxygen which arrives at the boundary. The direct influence of this geometrical parameter is felt to be small, but its value controls to some extent the char-holding capacity of the cavity, which can adjust transiently throughout the simulation. This char rubble volume in turn influences the ratio of outer to inner bed surface area, which determines the distribution of oxygen to the inner and outer beds. A relative increase in the inner bed oxygen rate results in taller, thinner cavities in which more overburden is rubblized and less combustible gas is recovered as a consequence. A key to the evolution of the cavity in this simulation is felt to lie in the size of the insulating char layer that builds up along the outer

Table 3

Effects of numerical parameters on results of simulations after 15 days. Input data values given in Tables 1 and 2.

run	total volume (m^3)	coal volume (m^3)	rock volume (m^3)	B-gas prod. (molx10^{-7})	cum. smoothing error (%)	h (m)	w (m)	CRAY-1 cpu time (sec)
num.0	835	466	369	2.28	-2.7	10.02	6.15	133
num.1	849	468	381	2.23	-2.6	10.14	6.13	83
num.2	862	469	393	2.19	-2.5	10.30	6.13	75
num.3	813	467	346	2.38	-2.3	9.74	6.19	247
num.4	792	474	318	2.47	-3.9	9.50	6.20	143
num.5	839	476	363	2.33	-2.5	9.78	6.27	147
num.6	868	457	411	2.08	-2.4	10.62	5.95	130
num.7	810	474	336	2.42	-2.3	9.57	6.29	140
num.8	761	440	321	2.35	-5.4	10.04	5.72	80
num.9	874	480	394	2.22	-1.1	10.03	6.33	384
ini.1	826	480	346	2.36	-1.6	9.97	6.25	138
ini.2	851	448	403	2.16	-2.6	10.51	5.95	140

edges of the cavity, and further studies are called for to understand this and reduce the dependence of the geometrical parameter γ on the predicted results. The angle defining the interface between the char rubble and the void is related to the angle of repose of loose char, and thus is bounded within a relatively narrow range and is not considered to be an arbitrary parameter.

As a preliminary test of the utility of the model to predict actual field results, a simulation was run using coal and rock compositional data and operating injection flow schedules and compositions from the Partial Seam CRIP UCG field test (Hill et. al., 1985). Coal and overburden failure parameters and an initial cavity size were assumed, and no effort was made to optimize these choices by fitting results to the actual data. Figure 5 compares actual and calculated results for the ratio of combustible gas

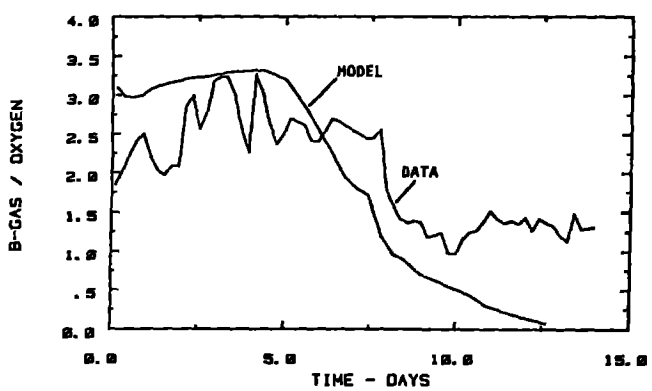

Figure 5. Comparison of model predictions of the ratio of combustible "B" gas produced to oxygen injected with data from the Partial Seam CRIP UCG field test conducted in Centralia, Washington in 1983.

produced to oxygen injected, a measure of the efficiency of the process. Qualitatively, the results are similar. The calculated value is somewhat higher than the data for the early part of the burn; this is probably due to water influx which was not included in the calculations. The model is capable of including a specified rate of water influx per unit cavity surface area, but cannot predict the amount of water influx a-priori. Inclusion of a rock rubble flow resistance, or inclusion of an outflow channel submodel would increase gas production rate during the later stages of the burn, thus bringing the model predictions closer to the measured results.

CONCLUSIONS

A UCG simulation model has been developed which is capable of describing the evolution of the full-seam consumption region of the cavity, assumed to be axisymmetric about an injection point low in the seam. The model is robust enough to simulate the entire lifetime of the cavity, and general enough to treat a wide variety of coal and rock stratigraphy and compositions, and operating conditions. The model relies on few arbitrary parameters, but employs some fundamental assumptions on the controlling mechanism for injection gas flow in the cavity, and on dominant heat and mass transfer processes in distinct regions of the cavity. Calculated results have been shown to be substantially independent of numerical or arbitrarily chosen geometrical parameters, and preliminary calculations have shown encouraging agreement with field test data. Development of the model is continuing, in particular development of additional submodels for coupling an outflow channel to model for the the main cavity considered in this report.

Model results show that the distribution of injection gas to various cavity regions controls the evolution of the cavity. It follows that the major assumption made by the model is that the ash formed around the injection source controls the distribution of this flow. Results obtained using this simple formulation are encouraging, but it remains to be demonstrated that it is a realistic assumption, and that it captures captures enough of the true physics to allow the

model in its present form to become a useful tool in further development of UCG technology.

Acknowledgments: *Support for this work was provided by Lawrence Livermore National Laboratory under the auspices of the U.S. Department of Energy, contract no. W-7405-Eng-48.*

NOMENCLATURE

A	gas species (=$H_2O + CO_2$)
A	surface area
B	gas species (=$H_2 + CO$)
C	heat capacity
F	gas flow
f_{ij}	radiant view factor between surfaces i and j
H	convective heat transfer coefficient
h	stream specific enthalpy
k	mass transfer coefficient
L	length
M_j	molecular or atomic weight of species j
P	pressure
Q	heat flow
Q_t	heat flow between subzones of wall model
$\bar{Q}$	heat required to dry and char a unit mass of coal
$\hat{Q}_j$	conductive heat flux into roof surface segment j
q_j	heat of reaction j
R	universal gas constant
r	radius
S	solid flow rate
T	temperature
v	surface recession velocity
w_j	weight fraction of species j in coal
w_j^*	weight fraction of species j in char
x_t	heat transfer parameter in wall model
Y_j	mole fraction of species j in gas phase
z	axial coordinate

Greek letters

α	fraction of spalled char onto outer bed which rolls into inner bed
γ	angle of ash rubble/char rubble interface, measured from horizontal
κ	permeability
μ	gas viscosity
ρ	density
σ	Stefan-Boltzmann constant
Ω	source strength of injection flow
Ψ	function describing location of permeable ash pile surface

Subscripts

A	A-gas
B	B-gas
C	carbon
ch	char
e	extinction conditions
f	failure conditions
i	injection conditions
ib	inner bed
ob	outer bed
O_2	oxygen
p	product
prt	particle
r	reaction zone in wall model
s	solid
w	water
v	volatile matter
<>	average value
∞	value at ambient coal conditions

REFERENCES

Aiman, W.R., H.C. Ganow and C.B. Thorsness, "Hoe Creek II Revisited: The Boundaries of the Gasification Zone" *Comb. Sci. Tech.* 23 125-130 (1980)

Britten, J.A. and C.B. Thorsness, Modeling Thermal and Material Interactions Between a Reacting Char Bed and a Gasifying/Spalling Coal Roof Proc. 11th UCG Symp. U.S. DOE rept. DOE/METC-85/6208 365-380 (1986)

Britten, J.A. "Recession of a Coal Face Exposed to a High Temperature" *Int. J. Heat Mass Transfer* (in press) (1986)

Britten, J.A, unpublished research (1985)

Chang, H.L., D.M. Himmelblau and T.F. Edgar, "A Sweep Efficiency Model for Underground Coal Gasification" Proc. 10th UCG Symp. U.S. DOE rept DOE/METC/85-5 460-476 (1984)

Dana, G.F., R.L. Oliver and J.R. Covell, "Evaluation of the Postburn Drilling, Coring and Geotechnical Surveying Program at the WIDCO-CRIP UCG Experimental Test Site, Centralia, Washington" Proc. 11th UCG Symp. U.S. DOE rept. DOE/METC-85/6208 9-36 (1986)

Gibson, M.A. and J.A. Wheeler, "Mathematical Modeling of Linked-Vertical Well In Situ Coal Gasification" Proc. 6th UCG Symp. Laramie Energy Tech. Cntr. rept. CONF 800716 III-1 (1980)

Grens, E.A. and C.B. Thorsness, "The Effect of Nonuniform Bed Properties on Cavity Wall Recession" Proc. 11th UCG Symp. U.S. DOE rept. DOE/METC-85/6208 413-423 (1986)

Grens, E.A. and C.B. Thorsness, "Wall recession Rates in Cavity Growth Modeling" Proc. 10th UCG Symp. U.S.

DOE rept. DOE/METC-85-7 448-461 (1985)

Hill, R.W., C.B. Thorsness, R.J. Cena and D.R. Stephens "Results of the Centralia Underground Coal Gasification Field Test" Proc. 10th UCG Symp. U.S. DOE rept. DOE/METC-85-7 11-26 (1985)

Krantz, W.B., D.W. Camp and R.D. Gunn, "A Water Influx Model for UCG" Proc. 6th UCG Symp. Laramie Energy Tech. Cntr. rept. CONF 800716 III-21 (1980)

Kunselman, L.V., D.W. Faucett and C.G. Mones, "A Comparison of Forward Combustion Gasification Models-II" Proc. 9th Underground Coal Gasification Symp. U.S. DOE rept DOE/METC/84-7, 182-195 (1983)

Riggs, J.B. and T.F. Edgar, "Sweep efficiency Models for Underground Coal Gasification: A Critical Asessment", in **Underground Coal Gasification: The State of the Art** W.B. Krantz and R.D. Gunn, eds., AIChE Symp. Ser. 226 V79 108-120 (1983)

Shapiro, A.B., "FACET - A Radiation View Factor Computer Code for Axisymmetric, 2D Planar and 3D Geometries with Shadowing" Lawrence Livermore National Lab. rept. UCID-19887 (1983)

Siegel, R. and J.R. Howell **Thermal Radiation Heat Transfer** 2nd ed. Hemisphere, Washington D.C. (1981)

Thorsness, C.B. and R.J. Cena, "An Underground Coal Gasification Model with Solids Motion" Proc. 9th UCG Symp. U.S. DOE rept. DOE/METC/84-7 246-281 (1983)

Wilks, I.H.C., "The Cavity Produced by Gasifying Deep Thin Seams" Proc. 9th UCG Symp. U.S. DOE rept. DOE/METC/84-7 314-322 (1983)

Youngberg, A.D., and D.J. Sinks, "Postburn Study Results for Hanna II Phases 2 and 3 Underground Coal Gasification Experiment" Proc. 7th UCG Symp. Lawrence Livermore National Lab. Rept. CONF-810923 18-28 (1981)